

Uncertainties in Coupled Thermal-Hydrological Processes Associated with the Drift Scale Test at Yucca Mountain, Nevada

S. Mukhopadhyay^{*}, Y. W. Tsang

Earth Sciences Division, E. O. Lawrence Berkeley National Laboratory, Berkeley, CA 94720, USA

Abstract

Understanding thermally driven coupled hydrological, mechanical, and chemical processes in unsaturated fractured tuff is essential for evaluating the performance of the potential radioactive waste repository at Yucca Mountain, Nevada. The Drift Scale Test (DST), intended for acquiring such an understanding of these processes, has generated a huge volume of temperature and moisture redistribution data. Sophisticated thermal-hydrological (TH) conceptual models have yielded a good fit between simulation results and those measured data. However, some uncertainties in understanding the TH processes associated with the DST still exist. This paper evaluates these uncertainties and provides quantitative estimates of the range of these uncertainties. Of particular interest for the DST are the uncertainties resulting from the unmonitored loss of vapor through an open bulkhead of the test. There was concern that the outcome from the test might have been significantly altered by these losses. Using alternative conceptual models, we illustrate that predicted mean temperatures from the DST are within 1°C of the measured mean temperatures through the first two years of heating. The simulated spatial and temporal evolution of drying and condensation fronts is found to be qualitatively consistent with measured saturation data. Energy and mass balance computation shows that no more than 13% of the input energy is lost because of vapor leaving the test domain through the bulkhead. The change in average saturation in fractures is also

^{*} Corresponding author. Fax: +1-510-486-5686; e-mail: SMukhopadhyay@lbl.gov

relatively small. For a hypothetical situation in which no vapor is allowed to exit through the bulkhead, the simulated average fracture saturation is not qualitatively different enough to be discerned by measured moisture redistribution data. This leads us to conclude that the DST, despite the uncertainties associated with open field testing, has provided an excellent understanding of the TH processes.

Keywords: Thermal; Hydrological; Drift Scale Test; Uncertainty; Coupled processes; Fractured rock; Radioactive waste; Yucca Mountain, Nevada

1. Introduction

The Yucca Mountain site at Nevada is currently being characterized to determine its suitability as a potential repository for high-level radioactive waste (HLW). Heat emanating from HLW, after its emplacement in the unsaturated zones of Yucca Mountain, is expected to produce coupled thermal, hydrological, mechanical and chemical (THMC) changes in the surrounding fractured tuff. For example, coupled THM changes may result in opening or closing of fractures, affecting fluid flow through them. Similarly, coupled THC processes may produce permanent changes in permeability, porosity, and other hydrological properties of the rock. These THC changes arise from mineral dissolution and precipitation enhanced by simultaneous transport of heat, fluid (water and gas) and vapor. To evaluate the performance of the potential repository, it is important to develop a good understanding of the various THMC changes associated with heating unsaturated rock. Of these coupled processes, understanding the TH processes is most critical because it is the driver for both the coupled THM and THC processes. In this paper, we shall focus our discussion on these TH processes.

TH coupling manifests itself in two kinds of data: temperature measurements and liquid saturation measurements. At the initial stages of heating unsaturated rock, most of the input energy goes into raising the temperature of the rock and the water residing in the pore spaces of the rock. This rise in temperature (of both the rock and the pore water) results predominantly from heat conduction, and effects of TH processes on the temperature signature are of a higher order. As heating continues, part of the pore water boils, and the vapor resulting from the boiling moves away from the source of heat. This vapor, reaching cooler regions of the host rock, then condenses. The continuous cycle of boiling and condensation results in large-scale moisture redistribution in the host rock. Changes in saturation in the host rock associated with these TH processes are difficult to probe and analyze. Active testing data, such as measurements of changes in fracture air-permeability or geophysical measurements like neutron logging (NEU), ground-penetrating radar cross-hole tomography (GPR) or electrical resistance tomography (ERT) provide useful information, though not entirely quantitative, about trends of saturation change in fractures and the matrix.

To acquire a more in-depth understanding of thermally driven coupled processes, a number of field thermal tests have either been completed or are being carried out at Yucca Mountain. Of all these thermal tests, the DST stands out as the largest *in situ* heater test ever undertaken. The heating phase in the DST began in December 1997 and continued till January 2002, for a total duration of little over four years. This heating phase is being followed by four years of cooling. Nine canister heaters placed on the floor of a Heated Drift (HD), 5 meters in diameter and 47.5 meters in length, provide heating in the DST. Fifty wing heaters located on the two sides of the HD provide additional

heating. Each of these wing heaters is installed in a 12 m long horizontal borehole drilled from the HD. They flank the entire length of the HD, see Figure 1 for a schematic representation of the position of the wing heaters with respect to the HD. The canister and wing heaters together provide about 185 kW of input heating power. Thermally driven, coupled THMC responses from the DST are monitored continuously by thousands of sensors installed in nearly 100 boreholes encompassing a rock block of 60 x 60 x 60 m³. Active testing is also being performed at regular intervals to capture the spatial and temporal evolution of moisture redistribution in the rock. A detailed description of the DST can be found elsewhere (Civilian Radioactive Waste Management System, CRWMS, 1998; Birkholzer and Tsang, 2000.)

Three-Dimensional (3-D) numerical models that take into account the realistic test geometry and all relevant TH processes (such as heat conduction, heat convection, boiling, vaporization, condensation, fluid flow in the matrix and fractures) have been developed for analyzing the large volume of TH data continuously generated from the DST. These models have been successful in predicting TH changes that compare well with the measured data (Birkholzer and Tsang, 2000). For example, the mean error between the simulated and measured temperatures from approximately 1,700 temperature sensors is reasonably small (a few degrees Centigrade after 30 months of heating). Also, the locations of dry-out and condensation zones deduced from ERT, GPR, neutron logs, and air permeability correlate well with the simulated time evolution of the liquid-saturation changes in the matrix and fractures. The good match between measured and simulated TH data from the DST (Birkholzer and Tsang, 2000) demonstrates that all the

major components of the TH processes are included in the models, and that we have gained a good level of understanding of the TH coupled processes.

Notwithstanding our confidence in the TH models, many uncertainties likely remain and need to be addressed. *In situ* field tests inherently contain more uncertainties than experiments carried out in the laboratory, where test conditions can be controlled. For the DST, for example, a source of uncertainty arises from the unmonitored quantity of vapor (and the energy associated with it) that may have left the test block through open boundaries. In particular, the hot side of the HD is separated from the unheated section by a bulkhead. This bulkhead, however, is not perfectly sealed because bundles of power cable and instrument-wiring pass through it. Therefore, a fraction of vapor generated in the rock mass from heating can enter the HD under a gas pressure gradient and then leave through the permeable bulkhead.

Other high-permeability conduits may also provide easy passage for vapor not into the cooler region of the test block, but instead into the HD and out through the bulkhead. The most likely candidates are the boreholes housing the wing heaters because of their direct connection to the HD and because of their proximity to the source of vapor production. The unmonitored loss of vapor through the bulkhead directly affects the amount of moisture that is retained in the test block and the measurements pertaining to moisture redistribution. Since vapor carries latent heat with it, the vapor loss also affects the spatial and temporal evolution of temperature within the test block.

In this paper, we focus on assessing the uncertainties in coupled TH processes associated with the DST. This paper is organized as follows. In Section 2, we present two alternative

conceptualizations. One is to consider the wing heater boreholes as having hydrological properties identical to the host rock, and the other is to treat them as high-permeability conduits. The uncertainties are assessed by comparing results from these two alternative models with measured temperature and moisture redistribution data. In Section 3 we present estimations of the partition of input energy into heating rock, heating water, and providing energy participating in phase changes. In Section 4, we provide a summary of our assessment of the impact of moisture loss through the open boundary on the fate of thermally mobilized water.

2. Assessment of uncertainties using alternative conceptual models

The welded tuff of Topopah Spring middle nonlithophysal (Ttpmn) stratigraphic unit (the host rock of the DST) is intensely fractured, with the continuum permeability of the well-connected fractures having a geometric mean of about 10^{-13} m^2 (Tsang et al., 2000), many orders of magnitude larger than that of the rock matrix. While part of the vapor generated by heating pore water in the DST is transported away from the source of heat into cooler regions of the host rock through this network of well-connected natural fractures, the remainder of the vapor is transported via the HD to the cool side of the bulkhead. Transport of vapor to the HD takes place through both natural fractures and high-permeability conduits of the wing heater boreholes. To assess the uncertainty associated with vapor loss, we consider two conceptual models of the DST. Both these models are based on a dual-permeability (DKM) conceptualization (Pruess, 1991), in which the rock matrix and the fractures embedded in it are modeled as two separate, interacting continua. Simulations for both these conceptual models are carried out using

the TOUGH2 simulator (Pruess, 1991). Both the conceptual models incorporate the bulkhead as an open boundary and the HD as a high-permeability conduit. In the first model (Birkholzer and Tsang, 2000), vapor transport to the HD is assumed to be mostly through the natural fractures in the host rock. That is, the wing heater boreholes are modeled as host rock. In the second model, the numerical gridblocks containing the wing heater boreholes are treated as high-permeability conduits. Both conceptual models have the same average total power input as the test. The same thermal and hydrologic properties are used for both the models and these properties are listed in Table 1. The rationale behind this choice of property set can be found in Tsang and Birkholzer (2000).

2.1 Temperature

Statistical measures such as the mean error (ME) and root-mean-square error (RMSE) have been developed for comparing measured and simulated temperatures from the DST (CRWMS, 2000). For calculating ME and RMSE, temperature data measured by approximately 1,700 resistance temperature devices (RTD) installed in 26 boreholes are compared with model temperatures, which are spatially interpolated to the RTD locations. These 26 boreholes are each 20 m in length and form five radial arrays along the HD. In Table 2, ME and RMSE are shown at various times since the initiation of heating at the DST for the two conceptual models. Observe that, for both models, ME is positive almost all the times, implying that simulated temperatures are on the average larger than measured temperatures. This indicates that simulated results from both conceptual models predict more heat being retained in the test block than actually measured. Though the mean error for both conceptual models is positive, the magnitude is much smaller for the conceptual model that treats the wing heater boreholes as high-

permeability conduits. As an example, when vapor transport occurs mostly through the natural fractures, ME is more than 4°C by 18 months of heating. However, ME for the other conceptual model is less than 1°C at 18 months of heating and remains small even at later times. These results indicate that the wing heater boreholes indeed play a role in transporting additional vapor to the HD and out through the bulkhead, and the validation of alternative conceptual models for vapor loss against measured temperature has helped to reduce uncertainty in understanding temperature data from the DST.

2.2. *Fracture liquid saturation*

To investigate the impact of unmonitored vapor loss on moisture redistribution in the rock, we examine the simulated fracture and matrix liquid saturation and compare them to measurements. Figures 2a and 2b show the contours of fracture liquid saturation at 24 months of heating in a selected vertical plane through the HD for the two conceptual models. Figure 2a is for the scenario where vapor transport can take place mostly through the fractures. Figure 2b on the other hand is for the scenario where vapor transport is additionally possible through the wing heater boreholes as well. The vertical plane selected for showing the contours of fracture saturation is the one containing Boreholes 57-61. The relative position of Boreholes 57-61 with respect to the HD is shown in Figure 1. In Figure 2a, observe that a dry-out zone (of decreased liquid saturation from pre-heat ambient values) appears around the HD and the wing heaters. Outside the dry-out zone, there is a zone with considerable amount of “wetting” (increased liquid saturation from condensation). Observe also that the wetting is both larger in extent and magnitude below the HD than above. This asymmetric distribution of the wetting zone

above and below the HD is caused by gravity drainage in the fractures. Comparable patterns of moisture distribution in the fractures are also seen in Figure 2b. However, since additional vapor has left the system in this model via transport through the wing heater boreholes, wetting in the condensation zone in Figure 2b is somewhat less than that in Figure 2a.

The temporal and spatial evolution of moisture redistribution in the DST fractures caused by heating are tracked by periodic air-injection tests. The preheat liquid saturation is small in the fractures because of the much stronger capillary suction of the rock matrix. During heating, an increase in the fracture liquid saturation from condensation will be evidenced by a decrease in the local air-permeability value, as the relative permeability to air decreases with the presence of water. Each of the twelve hydrology boreholes (57-61, 74-78, and 185-186) is typically subdivided by high temperature packers into four zones. Each packed-off interval is equipped with sensors for temperature, pressure, and relative humidity. Air-injection tests were carried out in every zone before heating began. A complete set of air permeability tests continues to be carried out periodically in every zone during heating, at least once per quarter. Estimated air-permeability values derived from the pressure response to these air injection tests were normalized to their preheat values. Only changes greater than expected measurement error (~10%) were considered for the comparative analysis.

To illustrate how air-permeability test results can be utilized to track the redistribution of moisture in fractures, we show the permeability data in Boreholes 59-60 as a function of time in Figure 3. The vertical axis of Figure 3 is the measured air permeabilities,

normalized to their respective preheat values. The horizontal axis is the date of testing. From Figure 3, we see that a trend of steady reduction in permeability (as liquid saturation builds up) has been established in Zones 2 and 3 in Borehole 59. The other two zones (Zones 1 and 4) in that borehole also exhibit a decline in air permeability, though not as sharp as that in Zones 2 and 3. Also, observe that Zone 60-4 in Figure 3b registered a relatively large decline in air permeability albeit a slight increase in August 1998, whereas Zone 60-1 registered a modest drop. In addition, the air permeability at Zone 60-2 fell sharply early, but later maintained a low steady value. Zone 60-3 exhibited a sharp reduction at the early phases of heating, but began rising on February 1999, around 14 months of heating. The initial decrease in permeability in different zones is attributed to condensation of vapor. At early stages of heating, the dry-out zone is smaller in extent, and the condensation zone is located closer to the HD. As heating continues, the dry-out zone expands, pushing the condensation zone farther away from the HD. This accounts for the decrease in permeability occurring in Zones 2 and 3 of Borehole 60 at times earlier than in the corresponding zones in Borehole 59. As heating continues, those zones, that were previously located in the condensation regime, would now be in the dry-out regime. This accounts for the rise in normalized permeability in Zone 60-3 after February 1999 and in Zone 59-3 around April 2000. The subsequent fluctuation (decrease and increase of normalized permeability) in Zone 60-3 following 14 months of heating is attributed to filling and draining of water in the fractures caused presumably by heterogeneity. For both the conceptual models (though only the distribution of moisture at 24 months is shown in Figures 2a and 2b here), it has been generally observed that the

simulated locations of drying and condensation zones are qualitatively consistent with the measured pattern and times of increased and decreased air permeabilities.

A more quantitative picture emerges when we consider the magnitude of expected air-permeability reduction from the simulated changes in fracture liquid saturation in fractures. We have shown that the air-permeability at selected locations drops by as much as a factor of 4–5 from its pre-heat values (Figure 3). Figure 4 shows the gas-phase relative permeabilities as a function of liquid saturation for the fractures and matrix, based on the property set shown in Table 1. In the model where vapor transport occurs mostly through fractures, an increase of fracture liquid saturation from ambient 10% to a maximum of 50% in the condensate zone is predicted (see Figure 2a). Figure 4 indicates that for this range of increase in saturation, the gas-phase relative permeability in the fractures drops by approximately a factor of 4–5. This is consistent with the measured air-permeability reductions. When vapor transport occurs both through fractures and wing heater boreholes, simulation results show a change in fracture saturation from 10% to 40%. Figure 4 shows that, for this smaller range of liquid saturation reduction, the air-permeability reduction factor is still in the range of 4–5.

The above results indicate that the simulated trends of drying and condensation in the fractures from both conceptual models correlate well with those inferred from periodic air-permeability measurements. Further, both models give comparable magnitude of maximum air-permeability reduction consistent with observed results. This is because the TH coupled processes give rise to only small changes in fracture liquid saturation,

and the air-permeability data cannot distinguish between the two conceptual models over such a small change.

2.3. *Matrix liquid saturation*

Periodical geophysical measurements (such as ERT, NEU, and GPR) have been carried out at the DST to track the zones of increased and decreased water content in the rock matrix. These methods are useful for assessing qualitative changes, but do not provide direct and reliable measured value of the absolute liquid saturation or water content in the matrix. Therefore, trend in data for a particular location in the test domain, rather than absolute values, is the most useful information for validating conceptual models. To assess uncertainty in spatial and temporal evolution of matrix liquid saturation, zones of drying and wetting deduced from the geophysical measurements at specific times are compared with the simulated contours of matrix liquid saturation at those times.

As an example of such an assessment, contours of simulated matrix liquid saturation at 24 months of heating are shown in Figures 5a and 5b, for the two conceptualizations, respectively, in the plane of neutron-logging Boreholes 64-68. Figure 5a shows that there is a dry-out zone around the HD and the wing heaters. Outside this dry-out zone, both above and below it, there is a zone of condensate build-up. However, unlike that for the fractures (Figures 2a and 2b), the condensate build-up is more symmetric, with the build-up below the HD being only slightly stronger than above it. Figure 5b shows patterns of drying and wetting that are similar to those of Figure 5a; the only difference is that the condensate zone in Figure 5b is less wet than that in Figure 5a. The lower liquid saturation in the condensate zone in Figure 5b results from the extra vapor that has left

the test domain. These figures demonstrate that the two concept models describe the same TH processes. Difference between the two alternate conceptual models in this regard lies only in the magnitude of saturation change.

In Figure 6, we show a tomogram of saturation change from preheat ambient values derived from a crosshole radar survey taken at 692 days (approximately 23 months) since initiation of heating. Note the decrease in saturation around the HD and the wing heaters, and the increase in liquid saturation immediately outside the drier-than-ambient region. When comparing these measured changes with the simulated matrix liquid saturation in Figures 5a and 5b, we note that the simulated location of the dry-out and condensation zones is consistent with the measured pattern of moisture redistribution. However, the measured changes in saturation cannot distinguish between the two alternative conceptual models, because of the inherent qualitative nature of geophysical data and the small magnitude of the overall decrease in matrix saturation from vapor loss.

It appears that, although measured data can be used to reduce uncertainty in understanding the spatial and temporal evolution of temperature (as discussed in Section 2.1), the same cannot be said about moisture redistribution in either the fractures or in the rock matrix. Since the moisture data are not sensitive enough to discriminate between the two conceptual models, we shall address the uncertainty issues related to moisture distribution in the following section through energy- and mass-balance considerations.

3. Assessment of uncertainties using energy- and mass-balance considerations

In this section, energy and mass balance considerations will be used to assess uncertainties. Since the vapor that escapes the bulkhead via the HD is unmonitored, the uncertainty introduced by this unmeasured vapor loss on the spatial and temporal evolution of temperature and moisture redistribution (in the host rock) needs to be evaluated. Using an approach based on energy- and mass- balance, we shall now show that the loss of water mass in the form of vapor (and the associated energy) results from a small fraction of the total energy supplied to the host rock and that the resultant change in fate of moisture is not large enough to be detected by measured data. These considerations will lead us to bracket the impact of unmonitored vapor loss on temperature and redistribution of moisture in the host rock.

3.1 Energy balance

This subsection addresses partitioning of input energy to the test block into respective functions: heating rock, heating water, and providing energy for phase change. If we consider a rock of volume 1 m^3 with thermal and hydrological properties as defined in Table 1, it is straightforward to show (based on the thermal conductivity of rock and water, and the porosity and liquid saturation of the fractured welded tuff) that, for single-phase conditions at below boiling temperatures, about 82.7% of the input energy goes into heating rock, while the remaining 17.3% goes into heating water. In other words, for the Yucca Mountain fractured welded tuff, the energy spent to heat the rock is approximately five times as large as that for heating water. This number is similar to what was determined by Freifeld (CRWMS, 2001) in an estimate of the global energy balance in the DST based on TOUGH2 simulation results. Since the average input energy to the

DST over the first 27 months of heating was approximately 185 kW, the expected energy required for heating the rock, based on the above rough estimate, is about 153 kW.

This finding is confirmed by Figure 7, where we show the total energy used in heating rock for the two models through the first 27 months of heating. Figure 7 is based on detail calculations incorporating the simulated temperature for every gridblock from the 3-D numerical model of the DST. Figure 7 shows that, during the first three months of heating when single-phase conditions generally prevailed in the test block, energy utilized in heating rock (151 and 153 kW respectively from the two conceptual models) is virtually identical to the simple estimation of 153 kW. The fraction of energy utilized in heating rock decreases gradually with continual heating, as temperature in large volume of rock approaches the boiling point of water and more heat is used for phase change of water into vapor. In addition, energy utilized in heating rock for the two different models is comparable, the difference in energy utilized in heating rock between the two models is not more than 10 kW. The point to note is that the majority of the heat input (74-81%, depending on the time elapsed since heating started) goes into raising the rock temperature. The loss of heat associated with the unmonitored escape of vapor has to come out of the balance (~ 20%) of the input energy. The uncertainty resulting from vapor loss, therefore, is rather small in terms of percentage of input energy.

To partition this balance (~20% of the input energy) into energy for heating water and for phase change, and to calculate that part of energy that exits the test domain in the form of vapor is not as easy as determining the energy required for heating rock. This is because rock has a constant mass, while the total mass of water available for heating changes with

time in a field test that has open boundary conditions. Freifeld (CRWMS 2001) made an attempt to determine the partition of energy for the TH processes, based on some simplifying assumptions. We (in the following) take a more indirect approach. Based on the simulated results for the 3-D numerical model, we first determine the decrease in mass of water in the rock matrix and the increase in mass of water in the fractures with progress of heating. We also determine the increase in mass of water vapor inside the test block.

For calculating these changes in water- and vapor-mass, a part of the model domain located within a radius of 60 m from the center of the bulkhead is chosen. The choice of the volume (which is much smaller than the total model domain for the DST numerical model) is based on the rationale that little change in temperature and saturation occurs beyond this selected volume. In addition, all measurement instruments are located within this selected volume. If we sum up the decrease in water mass in the matrix, the increase of water mass in the fractures and the increase in the mass of vapor, we obtain the total amount of pore water displaced by boiling from this chosen volume of welded tuff. The energy necessary to boil this water can then be easily calculated by multiplying the mass of water boiled with the latent heat of vaporization of water (2261 kJ/kg). These computations are performed for partition of input energy in coupled TH processes for the two conceptual models, and the results are shown in Figure 7. Figure 7 shows that no more than 24 kW (or a maximum of 13%) of input energy goes into vaporizing water during the first 27 months of heating in the DST. Having individually determined the heat used in heating rock (74–81%) and providing latent heat (maximum 13%), it can now be said that no more than 6–13% of the energy went into heating water from ambient

condition to boiling temperature. The 13% of input heat that went into boiling pore water provides an upper bound to energy loss associated with unmonitored moisture loss through the bulkhead.

3.2 *Water balance*

Since TH coupling is closely associated with moisture mobilization in the rock, it is important to assess the uncertainties associated with the fate of pore water. In assessing the uncertainty in fate of moisture, we focus mainly on saturation in the fractures rather than that in the matrix. This is because the change in saturation in the fractures, due to their small porosities and fast gravity-driven flow of condensate through them, is more than that in the matrix.

To develop an estimate of the change in the saturation of the fractures with progress of heating, we did the following. For each of the models, within the selected model subdomain, we computed the number of numerical gridblocks that exhibited an increase in fracture liquid saturation from their ambient (before heating) saturation. Using the simulated fracture saturation at three months of heating, we grouped the fractures into bins based on the magnitude of increase in saturation, such as what fraction of the fractures has an increase in saturation of 0.01 and less, what fraction has 0.05 and less, and so forth. The calculations were repeated for conditions at different times of heating, at an interval of three months. The results from such an analysis are shown in Figure 8 for the two models at 24 months of heating. Figure 8 shows that, of those fracture elements that showed an increase in saturation, an overwhelming majority has only a small increase. For example, when transport occurs mostly through fractures, almost 88% of

the fracture elements shows an increase of less than 0.2 from their ambient liquid saturations. Similarly, when wing heater boreholes also participate in transport of vapor, close to 92% of the fractures shows a change of less than 0.2 from their ambient saturation values. Only a small percentage of the fracture elements (about 1%) shows any appreciable change (0.3 or more) in saturation for both conceptual models. These small changes in moisture distribution demonstrate that the magnitude of uncertainty is small with regard to the fate of moisture in the DST, in spite of the inherent vapor loss.

There is another way of presenting the same results. Let us assume that all the water present in fractures was evenly distributed among all the fractures in the selected model domain. This would result in an ambient average saturation of approximately 7%. Average fracture saturation would then be calculated for the DST at different phases of heating at an interval of three months, for both the models. Figure 9 shows this average saturation at various times during heating at the DST. Observe that, on an average, the fracture saturation changes very little from their ambient conditions of 7% to 10.7% and 9.1% for the two models, respectively. This confirms that the magnitude of uncertainty associated with moisture transport is rather small.

3.3 *Water balance in a hypothetical closed system*

To further examine the impact of unmonitored vapor loss on TH coupling, we pose the following hypothetical question: What would be the redistribution of moisture if the DST were to be an ideally closed system and moisture were not allowed to escape the system at all? Assuming that no moisture left through the bulkhead, we made the entire mass of water displaced from the matrix available to the fractures. Based on this hypothetical

situation, we spread the water evenly in all fractures and recalculated the “average” fracture saturation. The hypothetical fracture saturation for the two alternate conceptual models are shown in Figure 9. Understandably, the estimated fracture saturation in the condensation zone for this hypothetical system is higher (maximum 31% and 33% for the two models, respectively, at 27 months) than that for the real test (10.7% and 9.1% for the two models, respectively, at 27 months), which include moisture loss. However, the maximum difference between the average fracture saturations at any time is less than 0.2. This is in a way a measure of the effect of open boundaries on the fate of pore water (and TH coupling). It has been shown earlier (see Figure 4) that the resulting change in air permeability arising out of such a change in fracture saturation would not have been detected by active hydrological testing. Therefore, it can be concluded that the DST has afforded us a very good understanding of the coupled TH processes, and the unmonitored loss of vapor through the bulkhead has not influenced the outcome of the test significantly.

4. Summary and conclusions

One source of uncertainty in the DST has been the unmonitored loss of moisture (and energy) leaving the test domain through an open bulkhead. To assess the uncertainty associated with vapor loss and to evaluate its impact on the outcome of the test, we used two alternative conceptualizations of the DST. In the first conceptualization, transport of vapor mostly through the natural fractures of the host rock was considered. In the second of the two conceptualizations, vapor transport through other high-permeability conduits, particularly through the boreholes housing the wing heaters, was also considered. We demonstrate that, as far as temperature rise is concerned, the second conceptualization produces results closer to measured data than the first

one. Similar sensitivity studies using alternative conceptual models were applied to moisture redistribution in both the fractures and the matrix. Measured spatial and temporal evolution of drying and condensation fronts in the fractures, as gathered from air-permeability testing, was qualitatively consistent with simulated locations of drying and condensation fronts for both the conceptualizations. The predicted range of reduction in air-permeability by both the models is consistent with measured air-permeability reduction. Air-permeability measurements therefore could not discriminate between two alternative conceptualizations. Similarly, geophysical measurements for monitoring moisture redistribution in the matrix provided qualitative trends of drying and wetting, which were consistent with predictions from both conceptualizations. It was concluded that the moisture data were not sensitive enough to distinguish between two conceptual models of vapor transport.

Uncertainties associated with the fate of moisture in the DST were evaluated using an approach based on energy and mass balance. We showed that almost 74–81% of the input heat energy in the DST went into heating rock. We also showed that about 6–13% of the input energy went into heating water. The rest (maximum 13%) of the input heat went into boiling the pore water. Since the energy loss (and vapor loss) through the bulkhead came out of this 13% of the input heat, in overall terms, the energy loss is small. To assess the impact of this unmonitored vapor loss on fate of moisture, we showed that almost 90% of the fractures showed a change of saturation of less than 0.2 from their ambient saturation. To further investigate the impact of unmonitored vapor loss on fate of moisture, we considered a hypothetical closed system where no vapor could leave the test domain through the bulkhead. The average fracture saturation in this hypothetical

situation would have been about 0.2 higher than that in the real test with open boundaries. Given the qualitative nature of measured saturation data, the difference in predicted average fracture saturation from the actual test and the hypothetical situation (~ 0.2) is not easily discernible.

Our assessment of uncertainties, in conjunction with previously published results showing good agreement between model predictions and measured data for the DST, has led us to conclude that the DST has provided greatly improved understanding of coupled TH processes. In summary, the DST has been invaluable in building confidence in our ability to properly evaluate the performance of a potential repository at Yucca Mountain.

Acknowledgements

We thank Philip Stauffer and an anonymous reviewer for critically evaluating the original manuscript. We also thank Nicolas Spycher and Dan Hawkes of the Ernest Orlando Lawrence Berkeley National Laboratory (LBNL) for their careful reviews of the manuscript. This work was supported by the Director, Office of Civilian Radioactive Waste Management, U.S. Department of Energy, through Memorandum Purchase Order EA9013MC5X between Bechtel SAIC Company, LLC and LBNL. The support is provided to LBNL through the U.S. Department of Energy Contract No. DE-AC03-76SF00098.

References

Birkholzer, J.T. and Tsang, Y.W., 2000. Modeling the thermal-hydrologic processes in a large-scale underground heater test in partially saturated fractured tuff, *Water Resources Research*, 36 (6), 1431-1447.

CRWMS M&O, 1998. Drift Scale Test As-Built Report, BAB000000-01717-5700-00003, REV 01, CRWMS M&O, Las Vegas, Nevada.

CRWMS M&O, 2000. Thermal Tests Thermal-Hydrological Analyses/Model Report, ANL-NBS-TH-000001 REV 00, CRWMS M&O, Las Vegas, Nevada.

CRWMS M&O, 2001. Thermal Test Progress Report # 6, CRWMS M&O, Las Vegas, Nevada.

Pruess, K., 1991. TOUGH2 – A General Purpose Numerical Simulator for Multiphase Fluid and Heat Flow, Technical Report LBL-29400, UC-251, Lawrence Berkeley National Laboratory, Berkeley, CA.

Tsang, Y.W., Huang, K., and Bodvarsson, G.S., 2000. Estimation of the heterogeneity of fracture permeability by simultaneous modeling of multiple air-injection tests in partially saturated fractured tuff, In: B. Faybishenko, P.A. Witherspoon, and S. Benson (Editors), *Dynamics of Fluids in Fractured Rocks: Concepts and Recent Advances*, Geophysical Monograph 122, American Geophysical Union, Washington D.C.

Figure Captions

Figure 1: Schematic diagram showing the Heated Drift, the wing heaters and the hydrology boreholes.

Figure 2a: Fracture liquid saturation at 24 months of heating in the plane of hydrology Boreholes 57-61 for the scenario where transport of vapor occurs mostly through fractures.

Figure 2b: Fracture liquid saturation at 24 months of heating in the plane of hydrology Boreholes 57-61 for the scenario where transport of vapor occurs both through fractures and wing heater boreholes.

Figure 3: Results of air-permeability measurements in hydrology Boreholes 59-60.

Figure 4: Gas-phase relative permeabilities in the fractures and the matrix used for simulations in the Tptpmn stratigraphic unit of Yucca Mountain.

Figure 5a: Matrix liquid saturation at 24 months in the plane of neutron logging Boreholes 64-68 for the scenario where transport of vapor occurs mostly through fractures.

Figure 5b: Matrix liquid saturation at 24 months of heating in the plane of neutron logging Boreholes 64-68 for the scenario where transport of vapor occurs both through fractures and wing heater boreholes.

Figure 6: Measured ERT saturation ratios and fraction water volume by neutron logging in the plane of Boreholes 64-68 at 692 days (approximately 23 months) of heating. The

black line around the heat source indicates the TOUGH2 simulated contour of 50% saturation.

Figure 7: Energy for heating rock and phase change as a function of time since initiation of heating in the DST.

Figure 8: Cumulative distribution of percentage of fractures exhibiting a particular increase in liquid saturation from their ambient saturation conditions for the two conceptual models at 24 months.

Figure 9: Estimated average fracture saturation for the two conceptual models. Also shown are the hypothetical fracture saturations for those conceptual models.

Table 1: Thermal and hydrological properties of the Topopah Spring middle nonlithophysal (Ttpmn) stratigraphic unit of Yucca Mountain used in simulations for both the conceptual models.

Name	Unit	TH property value	
		Fracture	Matrix
Permeability	m ²	0.1000e-12	0.1244e-16

Porosity	-	0.2630e-03	0.1100
van Genuchten α	1/Pa	0.9730e-04	0.2254e-05
van Genuchten m	-	0.4920	0.2469
Residual Liquid Saturation	-	0.01	0.18
Specific Heat Capacity	J/kg-K	952.9	952.9
Dry Thermal Conductivity	W/m-K	0.4392e-03	1.67
Wet Thermal Conductivity	W/m-K	0.5260e-03	2.00

Table 2: Comparison of statistical measures from the two conceptual models of vapor transport; ME is mean error and RMSE is root mean square error.

Time (months)	Measure (°C)	1 st Model	2 nd Model
6	ME	0.70	0.01

	RMSE	5.87	5.63
12	ME	2.41	-0.15
	RMSE	9.15	7.21
18	ME	4.24	0.90
	RMSE	11.15	8.72
24	ME	6.05	1.06
	ME	13.07	9.79

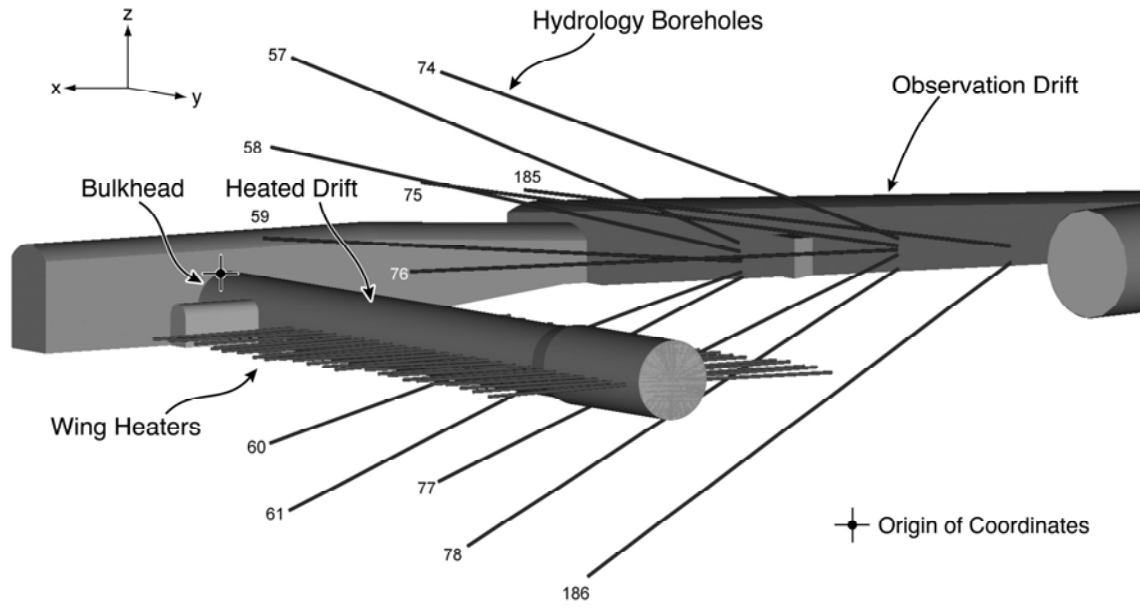


Figure 1

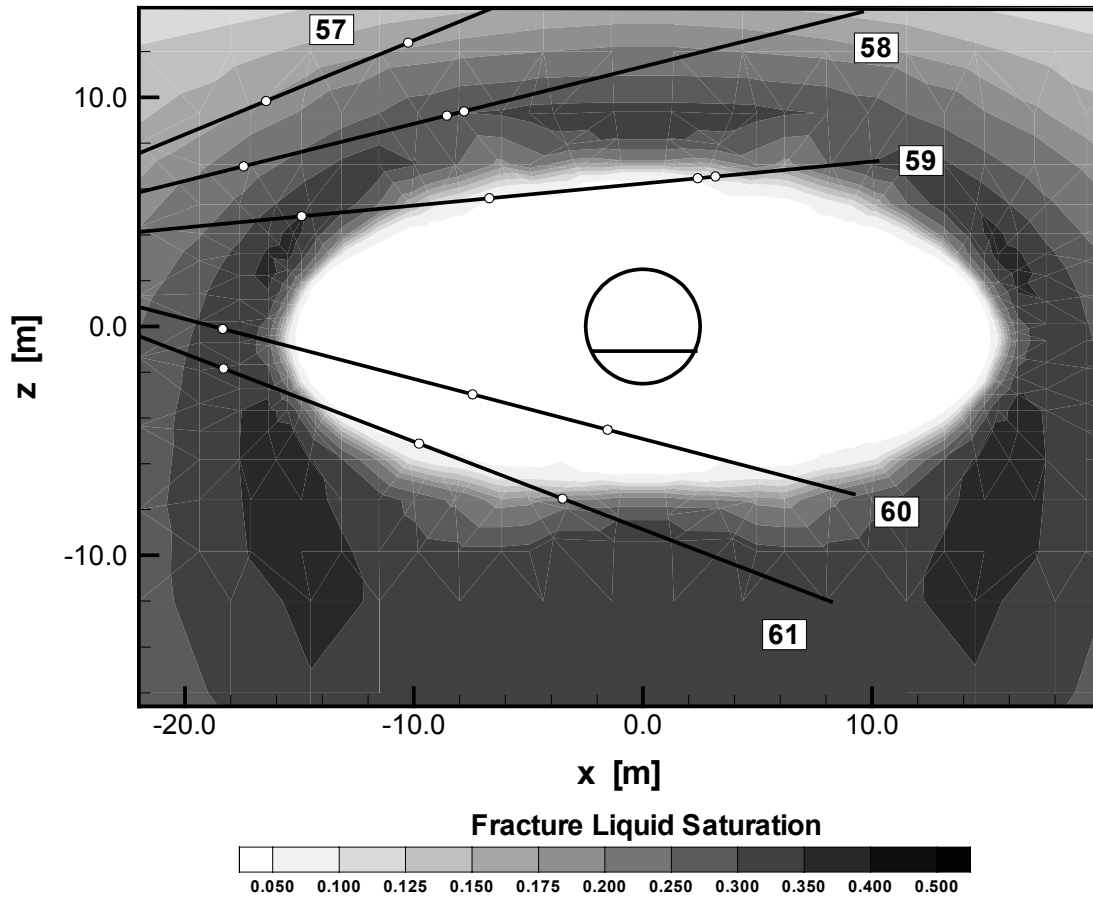


Figure 2a

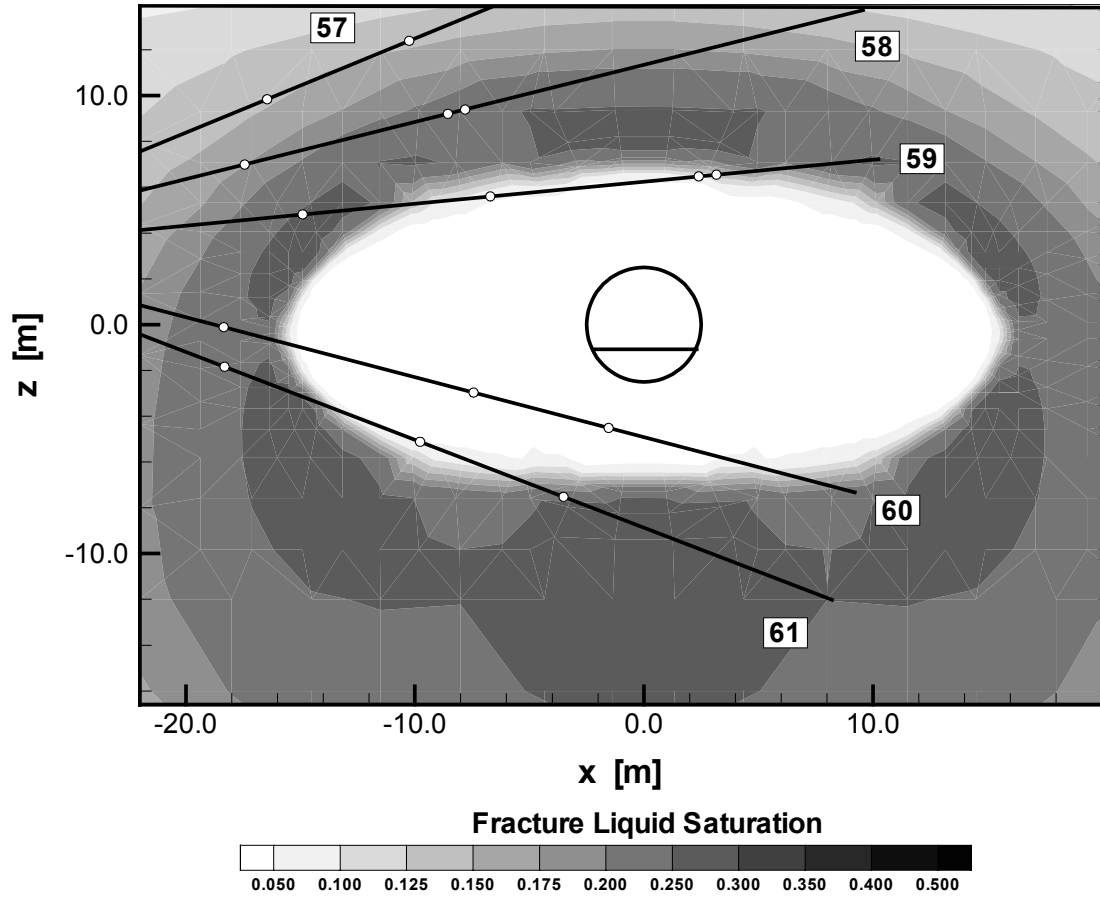


Figure 2b

Borehole 59-60

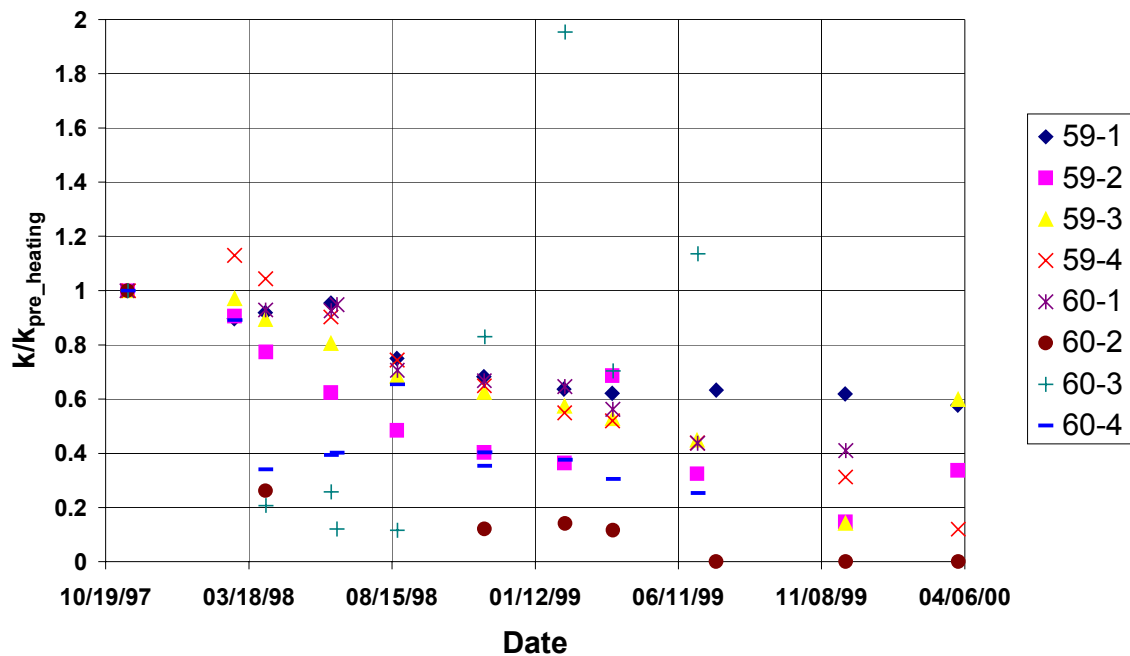


Figure 3

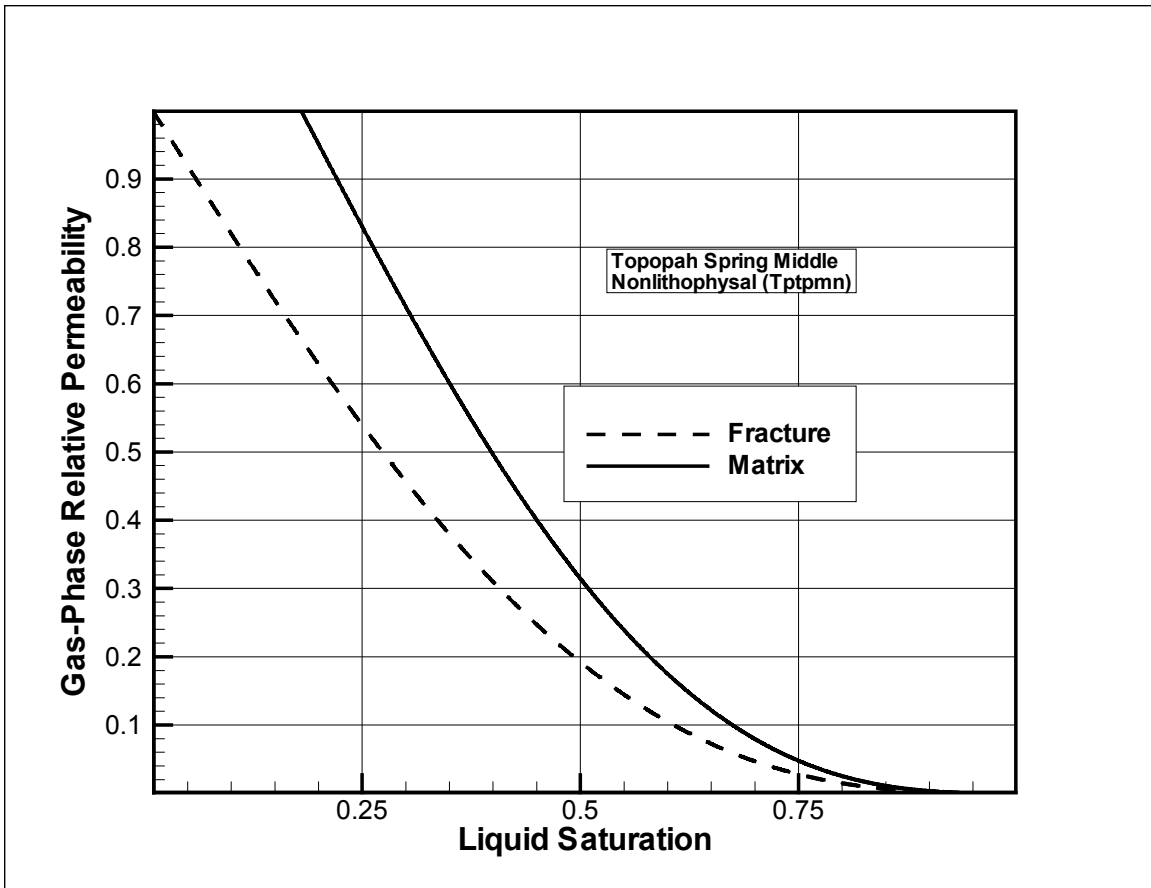


Figure 4

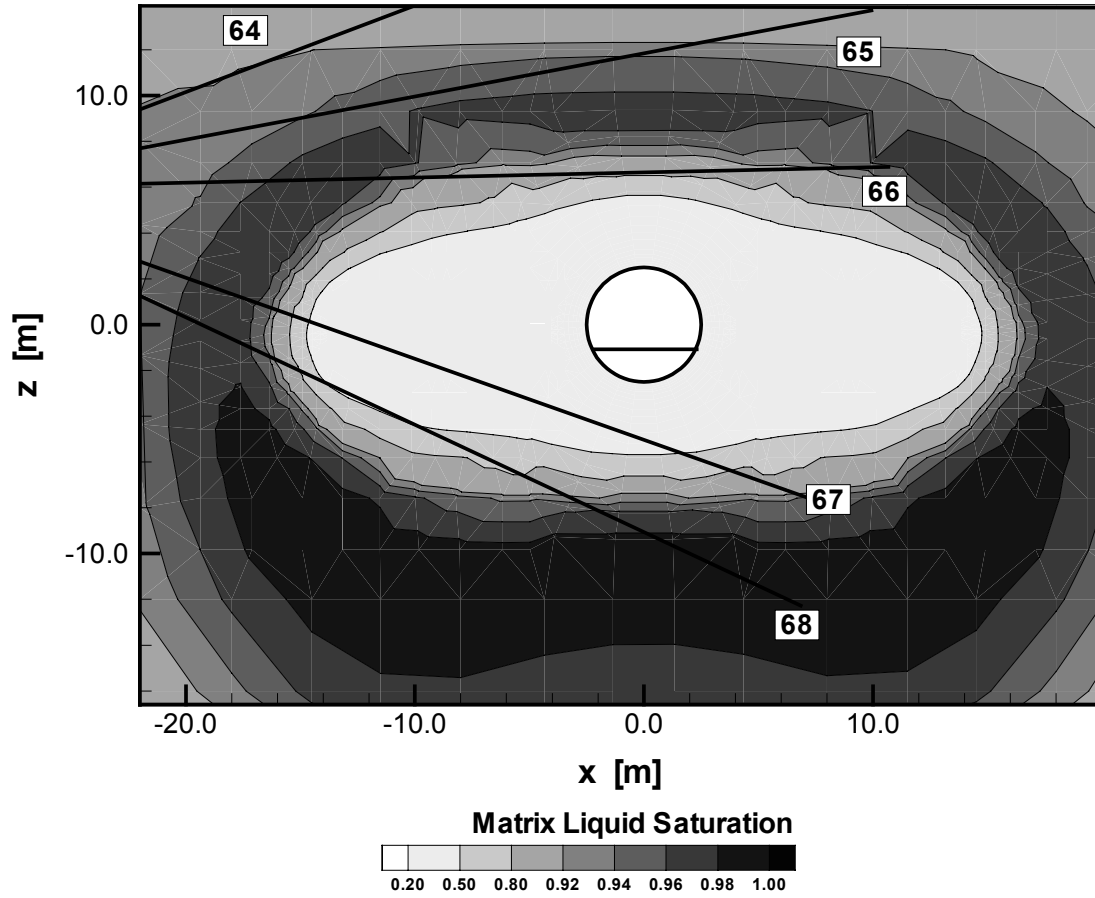


Figure 5a

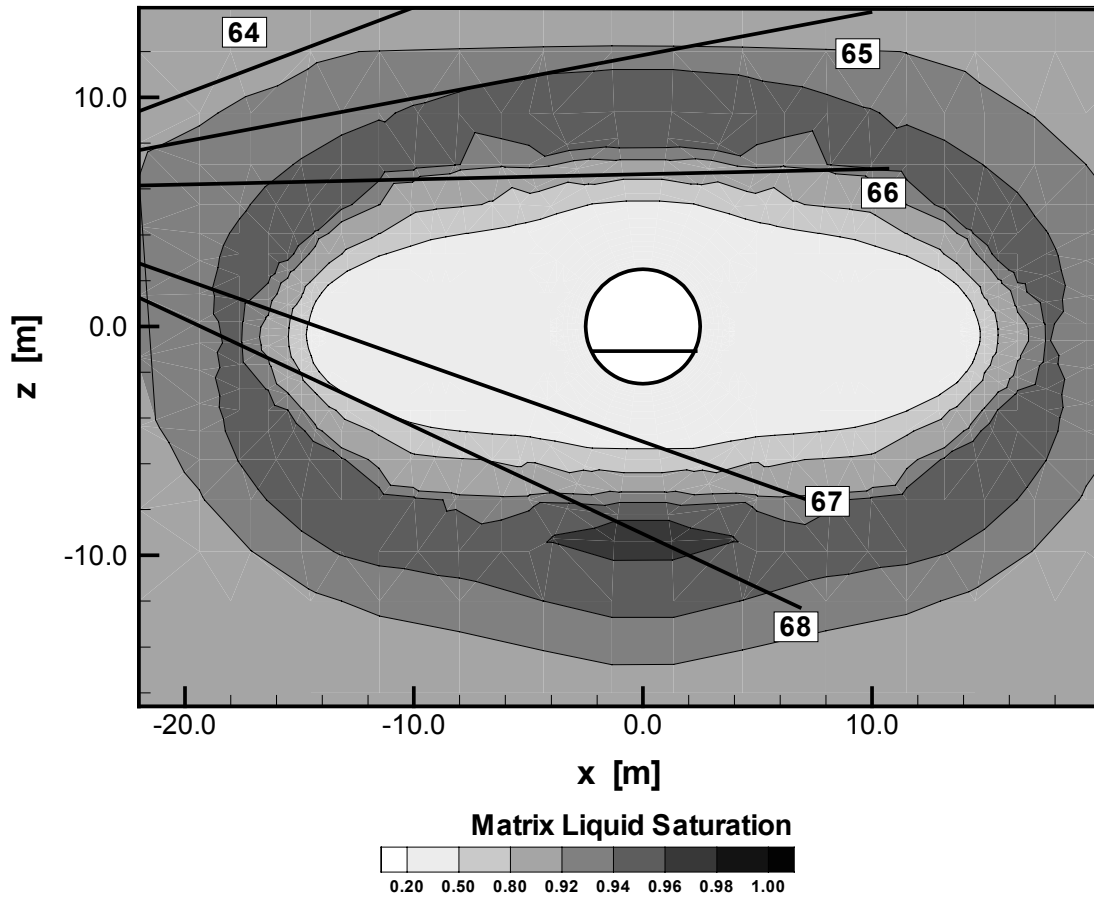


Figure 5b

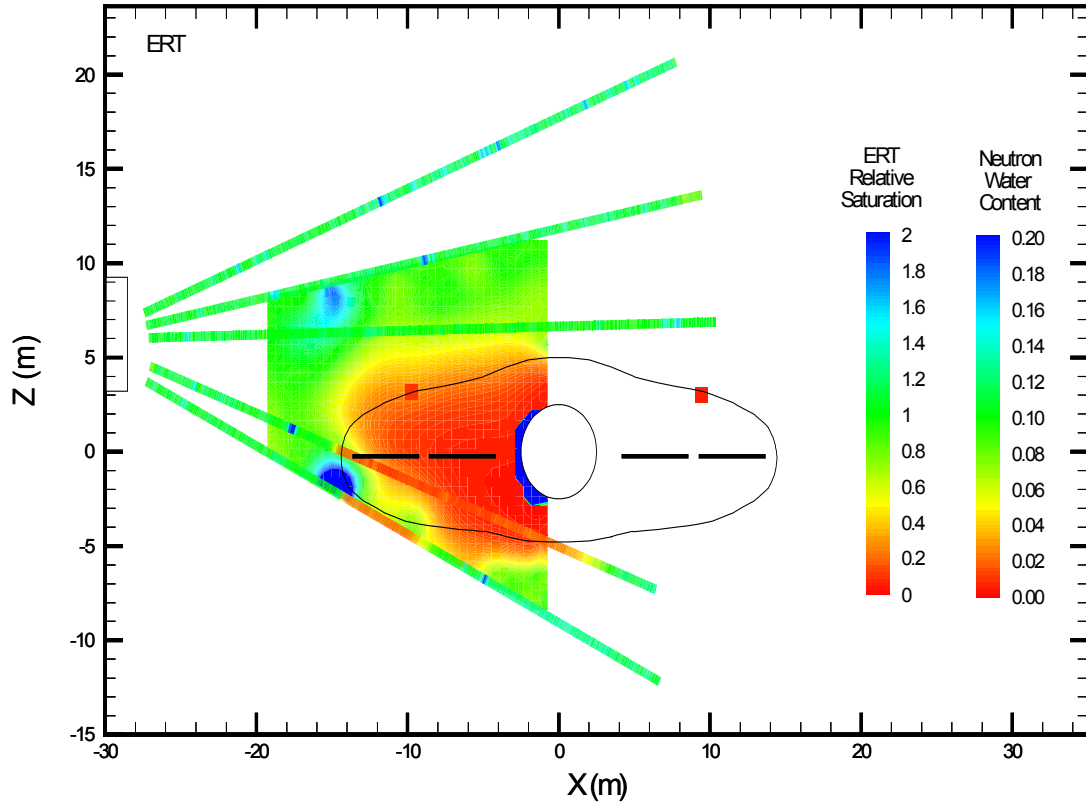


Figure 6

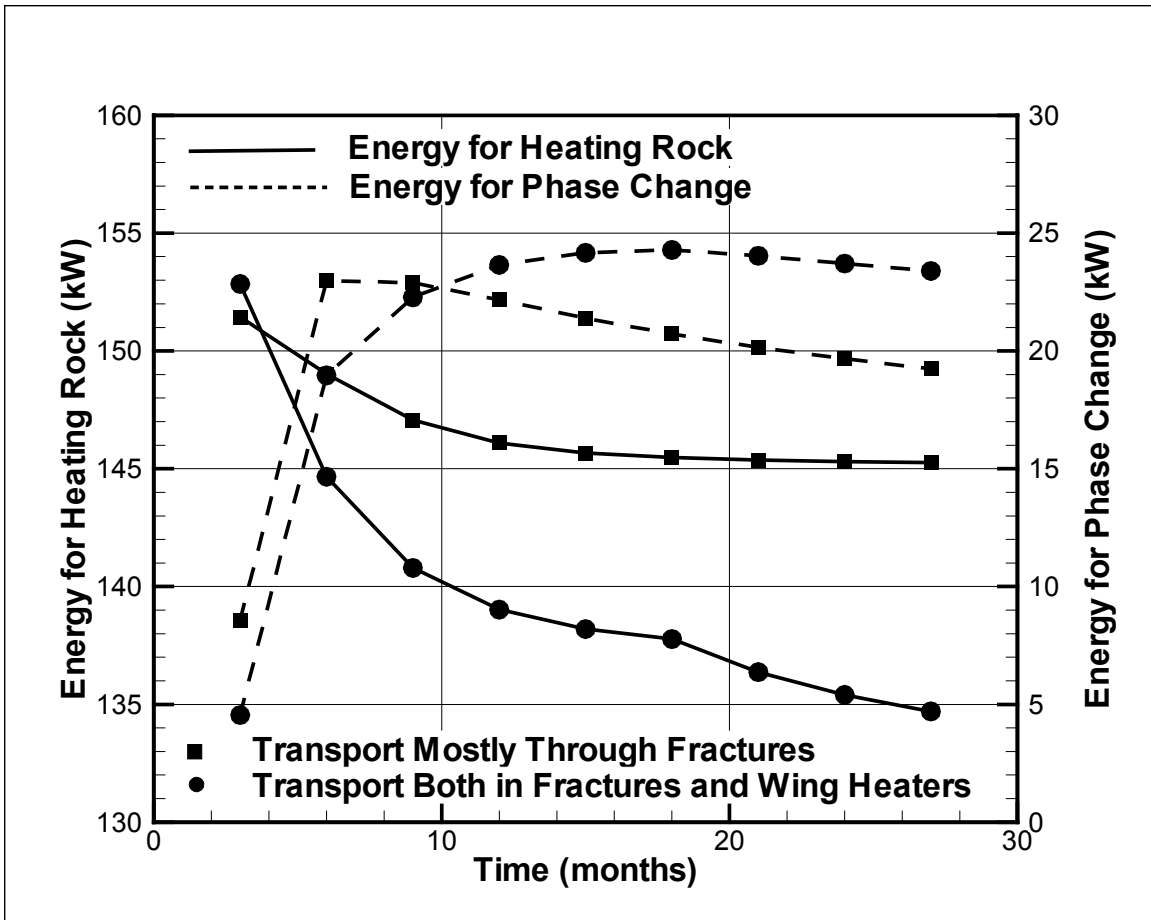


Figure 7

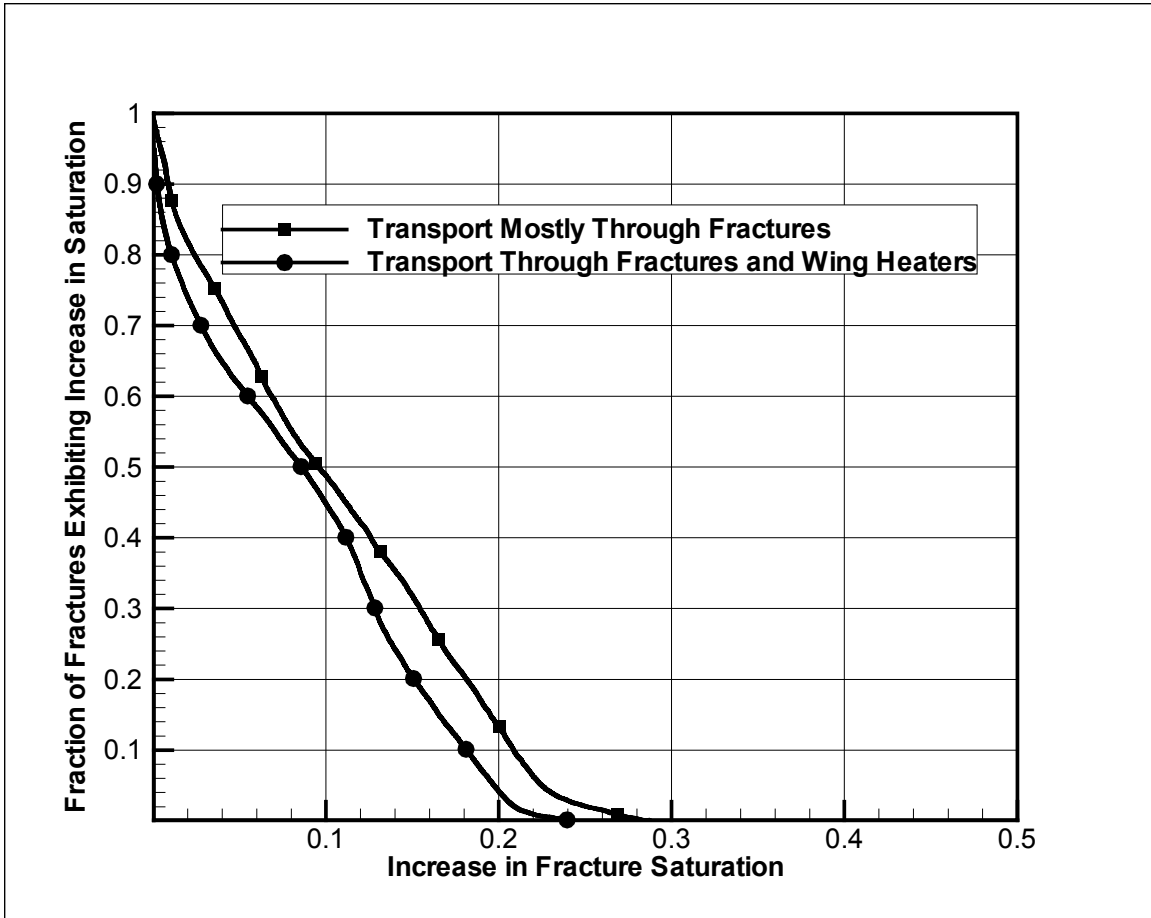


Figure 8

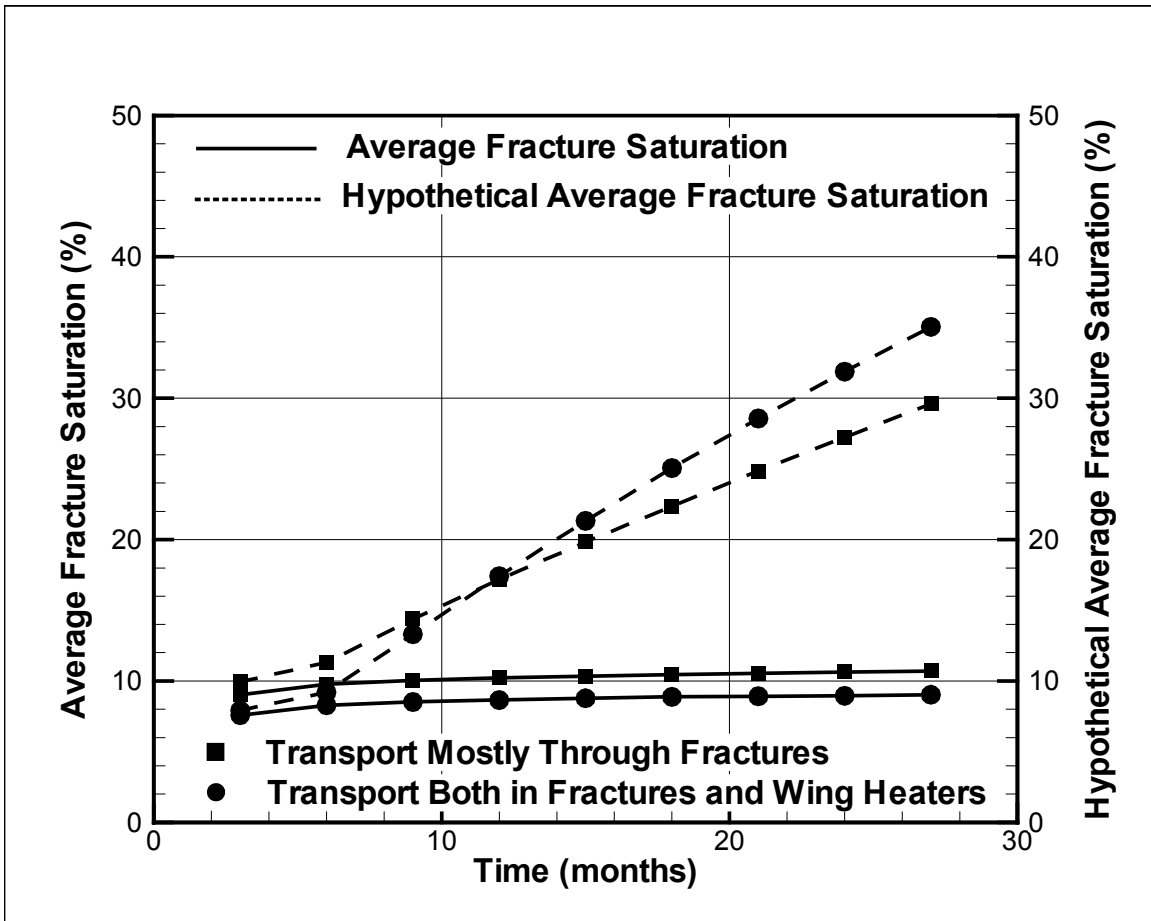


Figure 9

